Journal of Materials Chemistry

Cite this: *J. Mater. Chem.*, 2011, **21**, 14800

www.rsc.org/materials

PAPER

Nano-patterned monolayer and multilayer structures of FePtAu nanoparticles on aluminum oxide prepared by nanoimprint lithography and nanomolding in capillaries†

T. Gang,‡[a] O. Yildirim,‡[bc] S. Kinge,[ad] X. Duan,[b] D. N. Reinhoudt,[bd] D. H. A. Blank,[c] G. Rijnders,*[c] W. G. van der Wiel*[a] and J. Huskens*[b]

Received 12th April 2011, Accepted 21st July 2011
DOI: 10.1039/c1jm11559f

Owing to the superior dielectric property of aluminum oxide, precise patterning of self-assembled monolayers (SAMs) and nanoparticles (NPs) on aluminum oxide substrates is highly interesting for generating SAM- or NP-based electronic devices. This study employed nanoimprint lithography (NIL) and nanomolding in capillaries (NAMIC) for patterning ferromagnetic NPs on aluminum oxide substrates. We demonstrated the fabrication of structured arrays of various SAMs and NPs in micrometre and nanometre ranges. The polymer template generated by NIL behaved as a physical barrier and defined the pattern areas on the substrate. FePtAu NPs were assembled on phosph(on)ate SAM-modified polymer patterned substrates. After polymer removal, nano- and microscale line and dot NP patterns, with controlled layer thickness, were obtained on aluminum oxide substrates. Thick nanolines of NPs were obtained by NAMIC. PO_3-terminated FePtAu NPs were assembled on alumina without need of a linker. The magnetic properties of the NPs were addressed by vibrating sample magnetometry and those of the patterned NPs by magnetic force microscopy.

Introduction

Since the discovery of giant magnetoresistance and tunnel magnetoresistance in thin-film structures of alternating magnetic and non-magnetic layers, the field of spintronics has acquired massive scientific and industrial attention.[1] Driven by the need for higher integration density in magnetic and spintronic devices, spin-dependent transport in magnetic nanostructures has been extensively studied.[2,3] Most of the miniaturized spintronic devices were fabricated *via* top-down approaches involving metal/oxide deposition, lithography and etching, *etc.* Magnetic nanoparticle (NP) assembly potentially offers an alternative, cost-effective bottom-up approach to build nanoscale spintronic devices.[4–7] For instance, monolayers of magnetic nanoparticles can potentially replace the magnetic layers in conventional magnetic tunnel junctions. Moreover, magnetic nanoparticles may lead to ultra-small magnetic devices (ultimately down to the size of a single nanoparticle), thus offering high integration density.[8,9] To achieve this, it is essential to have a well-controlled patterning and assembly method to position the magnetic NPs on metal-oxide substrates, such as aluminum oxide which is widely used as the dielectric material in spintronics devices.[4,10–12]

Several attempts have been reported to address this issue, however those methods have their limitations. For instance, photo-patterned SAMs on metal oxides have been used to attach nanoparticles[13,14] and a contact printing method was demonstrated to create $Pt@Fe_2O_3$ core–shell nanoparticle patterns on silicon substrates.[15] In these cases, the dimensions, thickness and shape of the patterns are limited by the constraints of the fabrication process. In our previous study,[4] the directed assembly of nanoparticles on pre-patterned alumina substrates was introduced where the assembly of FePt NPs took place preferentially on the chemically active patterned regions. However, the selectivity was not optimal since some non-specific binding occurred on undesired areas as well.

[a]*NanoElectronics Group, MESA+ Institute for Nanotechnology, University of Twente, P.O. Box 217, 7500, AE, Enschede, The Netherlands. E-mail: w.g.vanderwiel@utwente.nl; Fax: +31 53 4893343; Tel: +31 53 4892873*
[b]*Molecular Nanofabrication Group, MESA+ Institute for Nanotechnology, University of Twente, P.O. Box 217, 7500, AE, Enschede, The Netherlands. E-mail: j.huskens@utwente.nl; Fax: +31 53 4894645; Tel: +31 53 4892995*
[c]*Inorganic Materials Science, MESA+ Institute for Nanotechnology, University of Twente, P.O. Box 217, 7500, AE, Enschede, The Netherlands. E-mail: a.j.h.m.rijnders@utwente.nl; Fax: +31 53 4893595; Tel: +31 53 4892618*
[d]*Supramolecular Chemistry & Technology, MESA+ Institute for Nanotechnology, University of Twente, P.O. Box 217, 7500, AE, Enschede, The Netherlands. Fax: +31 53 4894645; Tel: +31 53 4892980*
† Electronic supplementary information (ESI) available. See DOI: 10.1039/c1jm11559f
‡ First authors.

In this study, we demonstrate a robust approach to form patterned magnetic nanoparticle assemblies with high resolution and high selectivity on aluminum oxide substrates. Ferromagnetic NP patterns of micrometre and nanometre scale on aluminum oxide substrates were prepared by combining nanoimprint lithography (NIL) or nanomolding in capillaries (NAMIC) with self-assembled monolayers (SAMs). FePtAu and FePt NPs were used because they have a high chemical stability, a strong magnetocrystalline anisotropy, and a narrow size distribution.[16,17] Various PO_3-terminated molecular linkers were used to anchor the NPs onto alumina. Ferromagnetic properties of the NPs and NP patterns were addressed with a vibrating sample magnetometer (VSM) and magnetic force microscopy (MFM), respectively.

Experimental section

Materials

Polished substrates of R-(1–102) Al_2O_3 (1x10x10 mm) were purchased from SurfaceNet GmbH, Germany. These substrates were cleaned by ultrasonication in acetone and ethanol for 30 min each. Tetradecylphosphoric acid (TDP) was supplied by A. Wagenaar and J. Engbersen (RUG, Groningen). Phosphonoundecanoic acid (PUD, purity 96%), PMMA (weight-average molecular weight, Mw 350kD), N-[3-(trimethoxysilyl)propyl] ethylenediamine, $Pt(acac)_2$, oleic acid and silver enhancer solutions a and b were purchased from Sigma-Aldrich. Oleyl amine was purchased from Fluka. Hexadecanediol and iron pentacarbonyl were purchased from ABCR. Mercaptoundecylphosphonic acid (MUP) was synthesized according to a literature method.[18]

The syntheses of the FePtAu NPs and PO_3-terminated FePtAu NPs are based on modification of the procedures reported by Jia *et al.*[19] and Bagaria *et al.*[16,20] respectively. The details are described in the Supporting Information.

Nanoimprint lithography (NIL)

The molds were fabricated by photolithography followed by reactive-ion etching (RIE, Elektrotech Twin system PF 340) or by EBL followed by titanium evaporation and lift-off. They consisted of 5 μm wide lines at 15 μm period, 3 μm lines with 8 μm period with a height of 570 nm or 100 nm lines with around 4 μm period with a height of 125 nm.

1H, 1H, 2H, 2H-perfluorodecyltrichlorosilane was used as an anti-adherent layer to facilitate the stamp-imprint separation. Al_2O_3 substrates were cleaned by oxygen-plasma for 7 min and covered with a 460 nm thick layer of PMMA by spin-coating in case of micron size patterning. Stamp and substrate were put in contact and pressure of 40 bar was appliedat 180 °C using a hydraulic press (Specac). The residual layer was removed by dipping the samples in acetone for 25 s or by oxygen-plasma for 90 s using a RIE system. For nano patterns 120 nm thick PMMA and 18 s RIE was done. In the last step of NP pattern fabrication, the polymer layer was removed by 5 min acetone followed by 5 min chloroform immersion. For TDP SAM patterns, polymer layer was removed by 3 h ultrasonication in acetone. The imprint cycle was 30 min.

Monolayer patterning using NIL

PMMA paterned Al_2O_3 substrates were immersed into 0.125 mM TDP solution in 100 : 1 v/v hexane:isopropanol, a 1 mM PUD solution in 50 : 50 v/v ethanol : H_2O or a 0.5 mM mM MUP solution in ethanol for 2 days at room temperature. Afterwards, the samples were rinsed with the corresponding pure solvents or solvent mixtures, and dried under a flow of N_2.

Nanoparticle assembly

Al_2O_3 substrates covered with PMMA and self-assembled monolayer (SAM) patterns of PUD or MUP were immersed into a FePtAu (0.250 mg ml^{-1}) NP solution for 10–95 min to assemble NPs on the modified Al_2O_3 surfaces. For VSM measurements, fully MUP-covered Al_2O_3 substrates were immersed into a FePtAu (0.250 mg ml^{-1}) solution for 10 min. Subsequently the samples were rinsed with pure hexane to wash off physisorbed particles. After PMMA removal by acetone, patterns of NP monolayer was formed.

FePt NP multilayer patterns were prepared by using a concentrated solution of NPs. A drop of a 20 mg ml^{-1} solution of FePt NPs in hexane was deposited on the PMMA-PUD SAM-patterned alumina substrate. The sample was dried for 30 min under ambient conditions in a fume hood. The NPs precipitated on the surface upon evaporation of hexane and formed a multilayer due to the high concentration. Then the sample was gently immersed in acetone to remove PMMA without damaging the NP multilayer patterns.

Electroless deposition of Ag

The sample having FePtAu NP patterns attached to Al_2O_3 by MUP were immersed into a mixture of silver enhancer solutions for 20 min. Afterwards, the samples were rinsed with H_2O and ethanol, and dried under a flow of N_2. For the activation of SH end groups, a similar sample was immersed in $AgNO_3$ and $NaBH_4$ solutions for 1 min prior to Ag electroless deposition.

Nanomolding in capillaries (NAMIC)

Before NAMIC, the PDMS nanomold was shortly treated with oxygen plasma to to promote adhesion upon contacting the substrate.[21] 100 nm line features with 100 nm height was brought into conformal contact with PUD-functionalized alumina substrates. A drop of PO_3-terminated FePtAu NPs functionalized with MUP and dispersed in ethanol:Et_3N was put at one part of the PDMS for filling in the channels through capillary force. Here, FePtAu dispersed in hexane was not used since hexane causes swelling of PDMS which would cause non-uniform contact between the stamp and the substrate.

The sample was left for solvent evaporation and NP precipitation in the nano-channels. After 10 h the PDMS was removed, the residual polymeric material was rinsed with xylene followed by oxygen plasma and the substrate with line patterns of FePtAu was imaged by AFM and optical microscopy.

Measurements

Atomic force microscopy (AFM). The morphology of the nanoparticle-covered surfaces was observed by a digital

multimode Nanoscope III (Digital Instruments, Santa Barbara, CA) scanning force microscope, equipped with a J-scanner. All measurements were done at ambient in tapping mode, contact mode. The magnetic force microscopy (MFM) was done by a Dimension 3100 (Digital Instruments, Santa Barbara, CA). The MFM tips were provided by SmartTip (type SC-20-M). The approximate nanoparticle densities were calculated by counting particles in a certain area. A standard deviation of 5% was assumed based on our previous study.[4]

Contact angle (CA). Measurements were done with a Kruss G10 goniometer, equipped with a CCD camera. Contact angles were determined automatically during growth of the droplet by a drop shape analysis. Milli-Q water (>18.4 MOhm cm) was used as a probe liquid.

Vibrating sample magnetometry (VSM). Magnetic studies were carried out using a DMS Vibrating Sample Magnetometer (model VSM10) with fields up to 1500 kA m^{-1} and a sensitivity of 10^{-6} mAm^2. Measurements were done on NP assembly on MUP-modified Al_2O_3 substrate.

X-Ray diffractometry (XRD). The nanoparticle samples after annealing were analyzed by powder X-ray diffraction (XRD) analysis using a Philips X'Pert diffractometer (Cu-K$\alpha\lambda$ = 1.5418 Å).

High-resolution transmission electron microscopy (HRTEM-EDX). Particle sizes were analyzed by TEM (Philips CM-30 Twin operating at 200 kV voltage). A drop of hexane solution of the NPs was deposited on a carbon-coated copper grid.

Results and discussion

To prepare patterns of SAMs and FePt or FePtAu NPs on Al_2O_3 substrates, a combined NIL and self-assembly method was used. NIL enables high resolution and prevents non-specific assembly. The NPs were stabilized with the surfactants oleic acid and oleyl amine (Fig. 1). Oleyl amine binds to Pt through the amino group and oleic acid binds to Fe through the carboxylic acid group.[22] They can be replaced by other acids or amines, or by surfactants with a higher affinity to either Fe or Pt.[22] Thus, adsorbates with amine or carboxylic acid terminations were chosen (Fig. 1). By using FePtAu NPs prepared with solution annealing as described in ref. 4 instead of FePt, thermal annealing after assembling the NPs on the surface is not necessary to obtain ferromagnetic properties at room temperature, preventing possible aggregation which has been reported as a common problem due to thermal annealing.[23–25]

FePtAu nanoparticles

NPs were prepared by reduction of $Pt(acac)_2$ and Au(acac), decomposition of iron pentacarbonyl in the presence of oleyl amine and oleic acid surfactants and solution annealing, followed by precipitation of the NPs by using ethanol and redispersion in hexane. A drop of a solution of the NPs in hexane was deposited on a carbon-coated copper grid for TEM-EDX analysis. EDX analysis showed an elemental composition of $Fe_{57}Pt_{31}Au_{12}$. The particle size was determined by TEM to be ~4 nm (Fig. 2b). From Scherrer analysis from an XRD measurement made on a thick layer of FePtAu, a diameter of 3.56 nm was calculated, close to the TEM value (Fig. 2a) (NPs prepared by casting a 20 mg ml^{-1} FePtAu solution on a glass substrate followed by evaporation of the solvent without rinsing). FePtAu NP assembly on an MUP-modified Al_2O_3 substrate resulted in a monolayer coverage of NPs with a density of $(1.44 \pm 0.1)x10^{10}$ NPs/cm^2 (AFM not shown).

PO_3-terminated FePtAu nanoparticles (PO_3-NPs)

The PO_3-NPs were prepared from methyl-terminated FePtAu NPs (Fig. 1a) through ligand exchange with MUP (Fig. 1b) using a modification of the procedure reported by Bagaria *et al.*[20] The particles were dispersed in ethanol:Et_3N (10 : 1). The particle size is assumed to be the same as the FePtAu NPs (~4 nm).

SAM formation

The preparation and characterization of TDP, ABP and PUD monolayer-modified Al_2O_3 substrates have been discussed previously.[4] These monolayers, including MUP, were prepared according to literature procedures.[14,31–36] The water contact angle (CA) for MUP-covered Al_2O_3 was 87° similar to reported values.[36] Angle-dependent XPS measurements on MUP SAMs on alumina showed that the binding occurs *via* the PO_3 head-group (see Fig. S1, ESI‡). In conclusion, our measurements indicate the successful formation of the monolayers on alumina.

Magnetic properties of a full monolayer of FePtAu NPs assembled on a PUD SAM

FePtAu NPs assembled on an MUP-modified Al_2O_3 substrate were ferromagnetic, as studied by VSM. At room temperature a coercive field of 65 Oe was found (Fig. 3a). This is lower than previously reported values[16,26–28] probably due to the existence of a rich Fe phase in the FePtAu NPs, which forms a paramagnetic ion oxide shell around the FePt core.[29] FePt nanoparticles with ~4 nm diameter were prepared by a similar method as described previously.[4] The composition determined by XPS was $Fe_{48}Pt_{52}$. To investigate the effect of thermal annealing on the magnetic properties, a thick layer of FePt NPs was prepared by casting a 20 mg ml^{-1} FePt hexane solution on an alumina substrate followed by evaporation of the solvent. Then the sample was annealed under reducing conditions ($96\%N_2/4\%H_2$) for 1 h at 800 °C to transfer the NPs into the ferromagnetic $L1_0$ phase. The VSM measurements indicate the external maximal magnetic field was not strong enough to saturate the sample, thus the coercive field is larger than 10 kOe (Fig. 3b). This agrees with previously reported values, thus confirming the phase transformation. It is known that this high-temperature annealing procedure leads to a certain degree of clustering between neighboring FePt nanoparticles, since the organic ligands around the nanoparticles are destroyed at very high temperatures.[30]

SAM patterns prepared by NIL

Tetradecylphosphate (TDP) SAM lines were prepared as described in Fig. 1. The residual layer was removed by oxygen

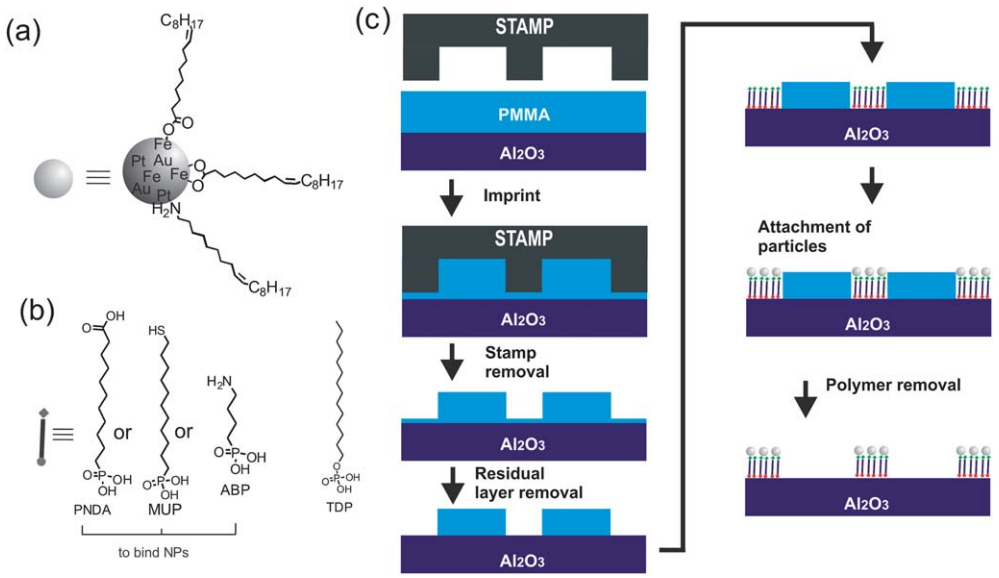

Fig. 1 (a) FePtAu NPs stabilized with oleic acid and oleyl amine. (b) The organic molecules used to attach NPs. (c) Patterns of NPs are formed by attachment through ligand exchange onto amino (aminobutylphosphonic acid, ABP), carboxylic acid (phosphonoundecanoic acid, PUD), and thiol (mercaptoundecylphosphonic acid, MUP) functionalized monolayer-modified substrates.

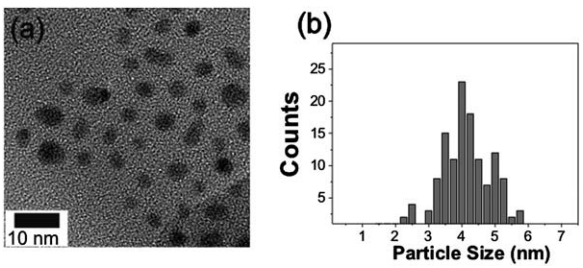

Fig. 2 (a) TEM image of FePtAu NPs. (b) Histogram of FePtAu NPs stabilized with oleyl amine and oleic acid.

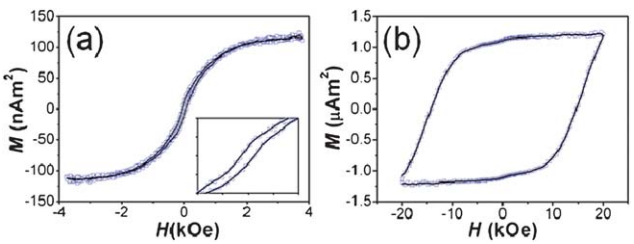

Fig. 3 (a) In-plane field hysteresis loop of FePtAu NPs assembled on an MUP-modified Al_2O_3 substrate. The inset of (a) is a zoom-in around zero field. The horizontal and vertical axis ranges are 0.25 kOe and 25 nAm^2, respectively. (b) In-plane field hysteresis loop of FePt NPs cast on an Al_2O_3 substrate after annealing.

plasma which enabled anisotropic etching and positive transfer of the mold features onto the substrate. A uniform TDP pattern was formed with homogeneous thickness, corresponding to one SAM layer (Fig. 4a). Nanopatterns of TDP SAMs were also prepared with a similar method but it was not possible to get a clear image probably due to the quite small size of the patterns. Alumina appears bright in the friction image (Fig. 4) because of a higher friction force relative to the TDP area. The TDP pattern was back-filled with N-[3-(trimethoxysilyl)propyl]ethylenediamine from gas phase to chemically pattern the substrate with two different kinds of SAMs. The friction force of the more hydrophilic NH_2-terminated area is higher compared to the CH_3-terminated TDP region (Fig. 4c).

Nanoparticle pattern preparation by NIL and SAMs

Fig. 5 shows the morphologies of the FePtAu patterns on Al_2O_3 substrates prepared by NIL and self-assembly as described in Fig. 1. PMMA was spin-coated on Al_2O_3 substrates with 460 nm

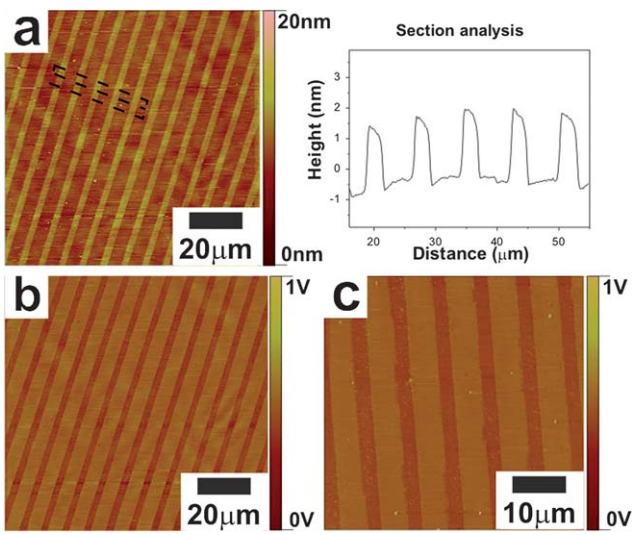

Fig. 4 Contact-mode height (a) and friction (b) AFM images of 5 μm lines of tetradecylphosphate (TDP) on Al_2O_3 with 8 μm period; (c) friction AFM image after subsequent evaporation of an amino alkyl silane. In the friction images, brighter areas indicate higher friction.

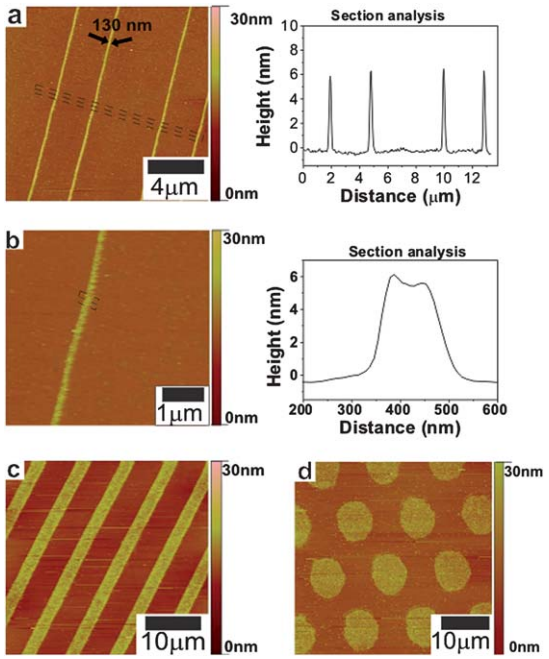

Fig. 5 Tapping-mode (TM) AFM height images of nanoparticles adsorbed on SAM-modified Al_2O_3 substrates. FePtAu nanoparticles, (a, b) 130 nm wide PUD lines, 10 min immersion, (c) 3 μm PUD lines, 10 min immersion, (d) 10 μm MUP dots, 10 min immersion.

and 120 nm thickness for micron and nanosize patterning, respectively. NIL was performed at a pressure of 40 bar at 180 °C. The residual layer was removed by oxygen plasma etching (RIE). The particles assembled on NH_2, SH and COOH terminated SAM patterns. Fig. 5 a,b shows that lines of FePtAu below 200 nm width formed by using a nano-mold and PUD as the linker. The heights of the FePtAu NP patterns were around 6 nm which shows a monolayer coverage. For the micron patterns, a similar height of FePtAu NP features was observed (not shown). An important advantage of nanoimprint lithography is the good edge definition. When compared to NP patterns prepared by using microcontact printing,[4] NIL patterns have well defined edges, and better contrast between patterned and bare regions. The FePtAu NP densities, calculated from AFM images, were similar for MUP and PUD-patterned surfaces, $(1.6 \pm 00.1) \times 10^{10}$ and $(1.5 \pm 00.1) \times 10^{10}$ NPs/cm^2, respectively. Since a similar coverage was reached with immersion time of 10 min for –SH and –COOH-modified surfaces, the relative rates of binding of NPs on modified surfaces are similar for MUP and PUD. The shape of the patterns are defined by the shape of the mold. As seen in Fig. 5d, dot patterns can also be prepared as well as lines. The lateral dimensions of the patterns were in good agreement with the feature size of the molds. The process is not limited to FePt NPs, any particle or molecule which has affinity to the end group of the SAM layer can bind to the surface to form a pattern.

Electroless deposition of Ag

Ag was grown by electroless deposition on NP patterns prepared by NIL and linked to Al_2O_3 by MUP. $AgNO_3$ and $NaBH_4$ solutions were used to deposit Ag ions and form SAg nucleation sites there to initiate Ag electroless deposition (Fig. 6a). In another experiment, Ag was grown directly, relying on possible surfactant free sites on FePtAu NP surfaces which would initiate the Ag electroless deposition (Fig. 6b). In both cases, a Ag layer of 30–60 nm was formed only in the patterned area with the FePt NPs. There was no Ag observed in the unpatterned area, which indicates a good selectivity of our patterning method.

Magnetic properties of multilayer of FePt NPs prepared by NIL

Magnetic force microscopy (MFM) is known to be a powerful technique for studying patterned magnetic structures.[15] It can effectively separate the magnetic from the topographical information of the sample. Due to the magnetic interaction between the magnetic dipoles of the sample and the oscillating tip, a phase contrast is observed which gives information on the magnetic state independent of the topography.[15] The phase contrast can be either positive or negative which corresponds to attractive or repulsive forces between the tip and the sample. Instead of a monolayer, a patterned FePt NP multilayer was used to have a strong enough magnetic signal for MFM measurements. Fig. 7 shows the AFM and corresponding MFM image of the FePt lines after annealing, which were recorded simultaneously. The height of the patterns was about 35 nm which corresponds to 8–9 layers of NPs and the width was around 5 μm (Fig. 7a). The magnetic contrast in the MFM phase image (Fig. 7b) is clearly visible and as expected, is not identical to the AFM height image (Fig. 7a). This is due to the random momentum directions of the NPs giving a non-homogeneous magnetic contrast. In other words, some NPs attract the magnetic tip while others repel it. The magnetization direction of the tip is perpendicular to the sample surface. At some regions the magnetic contrast is weaker than at other places which may be due to the small particle size, differences in coverage, or to the momentum direction of NPs being perpendicular to the magnetization of the tip.

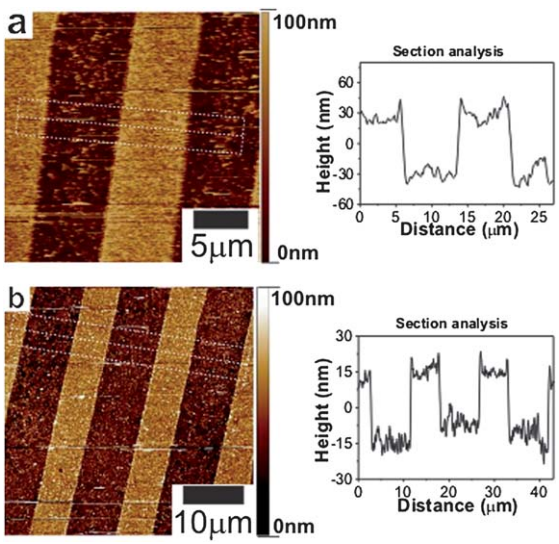

Fig. 6 Tapping-mode (TM) height AFM images of Ag lines prepared by electroless deposition on MUP-FePtAu patterns on alumina, by (a) forming SAg nucleation sites, (b) direct growth without activation.

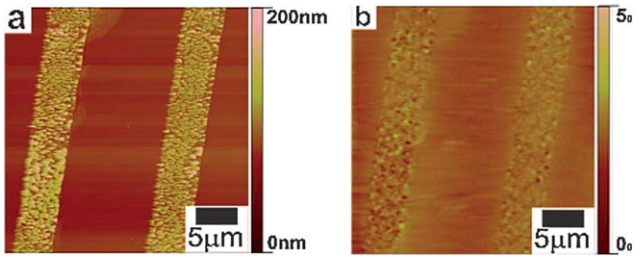

Fig. 7 AFM height (a) and MFM phase (b) images of FePt NP multilayer patterns after annealing under reducing environment (96%Ar/4% H_2) for 2 h at 800 °C.

Assembly of PO_3-terminated FePtAu NPs

MUP-stabilized PO_3-NPs (Fig. 8a) allow the direct assembly of NPs onto an Al_2O_3 surface without the need for a linker. PO_3-NPs are expected to bind to the alumina surface *via* the PO_3 head groups. Fig. 8 shows the morphology of the alumina sample after immersion in the PO_3-NP solution for 180 min. The NP density, calculated from AFM image, is $(4.2 \pm 0.2) \times 10^{10}$ NPs/cm^2. This is 5 times higher than the NP density for FePt on bare Al_2O_3 after 90 min immersion[4] which shows that the PO_3-NPs are probably attached to the surface through the PO_3 groups and that the high density is not due to non-specific adsorption. This kind of particles may be assembled on pre-patterned surfaces protected by methyl terminated regions to create NP patterns.

Multilayers of PO_3-terminated FePtAu NP patterns prepared by NAMIC

PO_3-NPs were used to create NP patterns on PUD-modified alumina, by nanomolding in capillaries (NAMIC), as illustrated in Fig. 9a. The main reason to use PO_3-NPs dispersed in ethanol + Et_3N is to prevent swelling of PDMS. Hexane was not used as a solvent, because it would destroy uniform contact and cause pattern deformation upon swelling. As seen in Fig. 9b,c continuous nanolines of FePtAu NPs were prepared without obvious defects over a large area. The shape of the pattern is in good agreement with the stamp used. The width of the NP patterns are close to the width of the nano-channels (Fig. 9e). Multilayers were achieved probably due to irreversible aggregation during drying. The height of the NP patterns was around 70 nm which corresponds to 15–20 layers of NPs. This value is lower than the nano-channel height (100 nm). This may be due to shrinkage after drying, to a low concentration of particles in the NP dispersion, or to the use of oxygen plasma on the mold before NAMIC. NAMIC enables to prepare densely packed NP multilayers, the height can be controlled by the height of the channels.

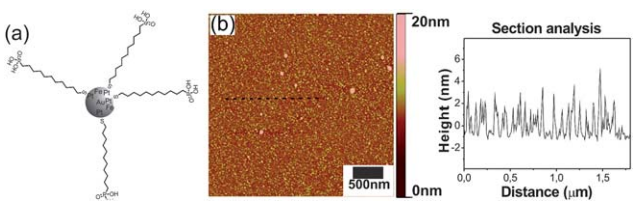

Fig. 8 (a) MUP-stabilized PO_3-terminated FePtAu NPs (PO_3-NP) (b) AFM image and section analysis of the PO_3-NPs assembled on a bare Al_2O_3 substrate after 180 min immersion.

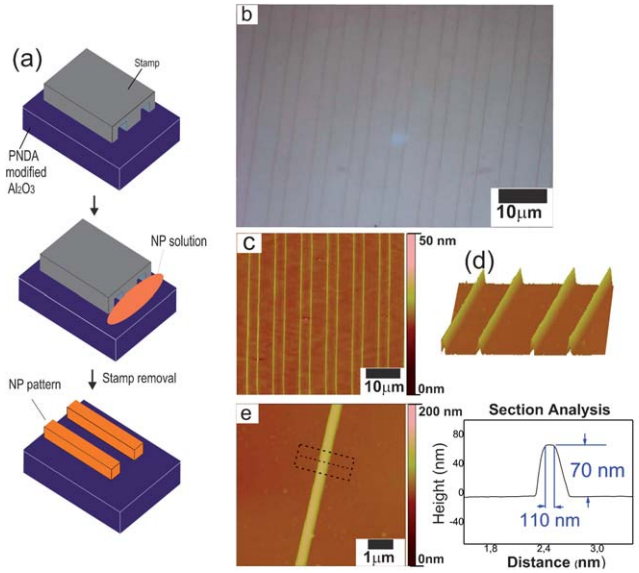

Fig. 9 (a) The NAMIC process. FePtAu patterns prepared by NAMIC on a PUD-modified alumina substrate, (b) optical image, (c,e) AFM height image with section analysis, (d) 3D AFM topography image.

Conclusions

By combining NIL or NAMIC with SAMs of phosph(on)ate molecular linkers, FePtAu NP mono/multilayer patterns with resolutions ranging from below 150 nm to the micron range have been demonstrated. High selectivity between the patterned and non-patterned regions was achieved. The ability to pattern magnetic nanoparticles at the nanoscale with high selectivity on metal oxide substrates can be considered as an important step towards the realization of ultra-small and cost-effective magnetic nanoparticle based spintronic devices.

Acknowledgements

The authors gratefully acknowledge support from the MESA+ Institute for Nanotechnology (SRO Nanofabrication) and NanoNed, the Nanotechnology network in The Netherlands. This work is part of WGvdW's research program 'Organic materials for spintronic devices', financially supported by the Netherlands Organization for Scientific Research (NWO) and the Technology Foundation STW. We acknowledge Mark Smithers for TEM and Gerard Kip for XPS measurements. We thank A. Wagenaar and J. Engbersen (RUG, Groningen) for providing TDP.

References

1 J. G. J. Zhu and C. D. Park, *Mater. Today*, 2006, **9**, 36–45.
2 Y. Okutomi, K. Miyake, M. Doi, H. N. Fuke, H. Iwasaki and M. Sahashi, *J. Appl. Phys.*, 2011, 109.
3 H. Tomita, T. Nozaki, T. Seki, T. Nagase, K. Nishiyama, E. Kitagawa, M. Yoshikawa, T. Daibou, M. Nagamine, T. Kishi, S. Ikegawa, N. Shimomura, H. Yoda and Y. Suzuki, *IEEE Trans. Magn.*, 2011, **47**, 1599–1602.

4 O. Yildirim, T. Gang, S. Kinge, D. N. Reinhoudt, D. H. A. Blank, W. G. van der Wiel, G. Rijnders and J. Huskens, *Int. J. Mol. Sci.*, 2010, **11**, 1162–1179.
5 S. Kinge, T. Gang, W. J. M. Naber, W. G. van der Wiel and D. N. Reinhoudt, *Langmuir*, 2010, **27**, 570–574.
6 S. Kinge, T. Gang, W. J. M. Naber, H. Boschker, G. Rijnders, D. N. Reinhoudt and W. G. van der Wiel, *Nano Lett.*, 2009, **9**, 3220–3224.
7 W. J. M. Naber, S. Faez and W. G. van der Wiel, *J. Phys. D: Appl. Phys.*, 2007, **40**, R205–R228.
8 C. T. Black, C. B. Murray, R. L. Sandstrom and S. H. Sun, *Science*, 2000, **290**, 1131–1134.
9 K. Liu, J. Nogues, C. Leighton, H. Masuda, K. Nishio, I. V. Roshchin and I. K. Schuller, *Appl. Phys. Lett.*, 2002, **81**, 4434–4436.
10 S. Yuasa, T. Nagahama and Y. Suzuki, *Science*, 2002, **297**, 234–237.
11 D. X. Wang, C. Nordman, J. M. Daughton, Z. H. Qian and J. Fink, *IEEE Trans. Magn.*, 2004, **40**, 2269–2271.
12 J. Schmalhorst and G. Reiss, *J. Magn. Magn. Mater.*, 2004, **272–276**, E1485–E1486.
13 H. Sugimura, A. Hozumi, T. Kameyama and O. Takai, *Adv. Mater.*, 2001, **13**, 667–670.
14 S. Q. Sun and G. J. Leggett, *Nano Lett.*, 2007, **7**, 3753–3758.
15 Q. J. Guo, X. W. Teng and H. Yang, *Nano Lett.*, 2004, **4**, 1657–1662.
16 S. Kinge, T. Gang, W. J. M. Naber, H. Boschker, G. Rijnders, D. N. Reinhoudt and W. G. van der Wiel, *Nano Lett.*, 2009, **9**, 3220–3224.
17 S. H. Sun, C. B. Murray, D. Weller, L. Folks and A. Moser, *Science*, 2000, **287**, 1989–1992.
18 T. R. Lee, R. I. Carey, H. A. Biebuyck and G. M. Whitesides, *Langmuir*, 1994, **10**, 741–749.
19 Z. Y. Jia, S. S. Kang, D. E. Nikles and J. W. Harrell, *IEEE Transactions on Magnetics*, 2005, 3385–3387.
20 H. G. Bagaria, E. T. Ada, M. Shamsuzzoha, D. E. Nikles and D. T. Johnson, *Langmuir*, 2006, **22**, 7732–7737.
21 X. Duan, Y. Zhao, E. Berenschot, N. R. Tas, D. N. Reinhoudt and J. Huskens, *Adv. Funct. Mater.*, 2010, **20**, 2519–2526.
22 S. H. Sun, *Adv. Mater.*, 2006, **18**, 393–403.
23 M. Acet, C. Mayer, O. Muth, A. Terheiden and G. Dyker, *J. Cryst. Growth*, 2005, **285**, 365–371.
24 T. W. Huang, Y. H. Huang, T. H. Tu and C. H. Lee, *J. Magn. Magn. Mater.*, 2004, **282**, 127–130.
25 T. W. Huang, K. L. Yu, Y. F. Liao and C. H. Lee, *J. Appl. Crystallogr.*, 2007, **40**, S480–S484.
26 J. W. Harrell, D. E. Nikles, S. S. Kang, X. C. Sun, Z. Jia, S. Shi, J. Lawson, G. B. Thompson, C. Srivastava and N. V. Seetala, *Scr. Mater.*, 2005, **53**, 411–416.
27 S. H. Sun, S. Anders, T. Thomson, J. E. E. Baglin, M. F. Toney, H. F. Hamann, C. B. Murray and B. D. Terris, *J. Phys. Chem. B*, 2003, **107**, 5419–5425.
28 A. C. C. Yu, M. Mizuno, Y. Sasaki, M. Inoue, H. Kondo, I. Ohta, D. Djayaprawira and M. Takahashi, *Appl. Phys. Lett.*, 2003, **82**, 4352–4354.
29 L. Savini, E. Bonetti, L. Del Bianco, L. Pasquini, L. Signorini, M. Coisson and V. Selvaggini, *J. Magn. Magn. Mater.*, 2003, **262**, 56–59.
30 I. Zafiropoulou, *et al.*, *Nanotechnology*, 2005, **16**, 1603.
31 E. S. Gawalt, M. J. Avaltroni, N. Koch and J. Schwartz, *Langmuir*, 2001, **17**, 5736–5738.
32 M. Gnauck, E. Jaehne, T. Blaettler, S. Tosatti, M. Textor and H. J. P. Adler, *Langmuir*, 2007, **23**, 377–381.
33 I. L. Liakos, R. C. Newman, E. McAlpine and M. R. Alexander, *Langmuir*, 2007, **23**, 995–999.
34 C. Messerschmidt and D. K. Schwartz, *Langmuir*, 2001, **17**, 462–467.
35 M. Textor, L. Ruiz, R. Hofer, A. Rossi, K. Feldman, G. Hahner and N. D. Spencer, *Langmuir*, 2000, **16**, 3257–3271.
36 J. Amalric, P. H. Mutin, G. Guerrero, A. Ponche, A. Sotto and J. P. Lavigne, *J. Mater. Chem.*, 2009, **19**, 141–149.